Received: 14 July 2023 | Accepted: 31 January 2024

DOI: 10.1002/aps3.11585

Applications in Plant Sciences

PROTOCOL NOTE

Carbon balance: A technique to assess comparative photosynthetic physiology in poikilohydric plants

Kirsten K. Coe[1] | **Nicolas Neumeister**[1] | **Maya I. Gomez**[2,3] | **Niko Carvajal Janke**[4]

[1]Department of Biology, Middlebury College, Middlebury, Vermont 05753, USA

[2]University of Southern California, Los Angeles, California 90089, USA

[3]Perry Institute for Marine Science, Waitsfield, Vermont 05673, USA

[4]Department of Viticulture and Enology, University of California Davis, Davis, California 95616, USA

Correspondence

Kirsten K. Coe, Department of Biology, Middlebury College, Middlebury, Vermont 05753, USA.
Email: kcoe@middlebury.edu

Abstract

Premise: Poikilohydric plants respond to hydration by undergoing dry–wet–dry cycles. Carbon balance represents the net gain or loss of carbon from each cycle. Here we present the first standard protocol for measuring carbon balance, including a custom-modified chamber system for infrared gas analysis, 12-h continuous monitoring, resolution of plant–substrate relationships, and in-chamber specimen hydration.

Methods and Results: We applied the carbon balance technique to capture responses to water stress in populations of the moss *Syntrichia caninervis*, comparing 19 associated physiological variables. Carbon balance was negative in desiccation-acclimated (field-collected) mosses, which exhibited large respiratory losses. Contrastingly, carbon balance was positive in hydration-acclimated (lab-cultivated) mosses, which began exhibiting net carbon uptake <15 min following hydration.

Conclusions: Carbon balance is a functional trait indicative of physiological performance, hydration stress, and survival in poikilohydric plants, and the carbon balance method can be applied broadly across taxa to test hypotheses related to environmental stress and global change.

KEYWORDS

carbon dioxide exchange, desiccation, hydration, infrared gas analysis, poikilohydry, precipitation

Across the plant kingdom, water availability can limit photosynthesis and fixation of atmospheric carbon (C) (Lawlor, 2002; Bota et al., 2004; Flexas et al., 2006; Green et al., 2019). Homoiohydric plants (most angiosperms, gymnosperms, and ferns) can regulate internal water content, and are thus capable of maintaining rates of C fixation through a wide range of environmental water availabilities (Tenhunen et al., 1990; reviewed in Lawson and Vialet-Chabrand, 2019). In poikilohydric plants (bryophytes, many ferns, and some angiosperms), internal water content varies, often rapidly equilibrating, according to availability from the surrounding environment (Proctor and Tuba, 2002). Depending on their habitat, poikilohydric plants experience periods of hydration and desiccation (anhydrobiosis) at different frequencies, ultimately going through a dry–wet–dry cycle whenever a pulse of environmental water becomes available. Such alternating periods between wet and dry tissue states can occur on a daily basis (Hamerlynck et al., 2000; Proctor, 2004; Asami et al., 2019), or may be as infrequent as several times a year (Stark, 2005; Jung et al., 2019). As operational photosynthetic machinery requires intracellular water, poikilohydric plants are thus only actively fixing C when hydrated. Because the rate of C fixation changes with plant water content (Proctor et al., 2007), such dry–wet–dry cycles are characterized by periods of C gain and loss (Mishler and Oliver, 2009; Coe et al., 2012). The net C uptake following such a cycle, referred to as the C balance, is a plant functional trait that is directly linked to desiccation tolerance (DT) (Coe et al., 2019), individual survival (Coe et al., 2012), and primary productivity (Coe and Sparks, 2014).

Originally referred to as the integrated water-driven carbon budget model (Mishler and Oliver, 2009), the pattern of C gains and losses during a dry–wet–dry cycle in a poikilohydric plant typically exists in three distinct

phases (Figure 1). First, upon rehydration from a desiccated state, the plant expends respiratory energy to reinstate metabolism and initiate transcription of DT-specific genes (Bewley, 1979; Oliver et al., 2004; Moore et al., 2009; Coe et al., 2012), resulting in a phase of net C loss (phase A). Second, once photosynthesis resumes in the hydrated tissues and the rate of C uptake outpaces that of respiration, an initial CO_2 compensation point is surpassed, and the plant enters a phase of net C gain (phase B). The time to CO_2 compensation point varies from 30 min or less in the desert mosses *Syntrichia caninervis* Mitt. and *S. ruralis* (Hedw.) F. Weber & D. Mohr (Tuba et al., 1996; Reed et al., 2012), to over 24 h in the DT angiosperm *Xerophyta scabrida* (Pax) T. Durand & Schinz (Tuba et al., 1998). When environmental water disappears and tissues dry out, cells are repackaged for desiccation based on either inducible or constitutive protection mechanisms (Oliver et al., 2005), the rate of photosynthesis once again drops below that of respiration, and a third phase of net C loss occurs (phase C). The size and shape of the three phases of the C balance curve as well as the total length of time for a given dry–wet–dry cycle depend on several factors, including the size of the precipitation event, the previous environmental conditions experienced by the plant, the time of year, and the trait-based adaptive strategies employed by individual poikilohydric species.

Carbon balance is considered a key functional trait for poikilohydric plants because it is reflective of individual physiology and survival (i.e., a response trait), as well as indicative of ecological processes at the community and ecosystem level (i.e., an effect trait) (Lavorel and Garnier, 2002; Stanton and Coe, 2021). Embedded within a C balance measurement are other important physiological response traits, such as the CO_2 compensation points (CCPs), the maximum light-saturated rate of photosynthesis (A_{max}), the rate of dark respiration (R_d or R_{max}), and rehydration/dehydration time (Figure 1). Additionally, C balance acts as an effect trait because positive C balance over time leads to C sequestration on landscape or ecosystem scales (Coe and Sparks, 2014), whereas negative C balance, if resulting in diminished performance or survival in keystone plants, can result in compromised community structure and function (Reed et al., 2012).

Variation in C balance can be attributed to evolutionary history (Coe et al., 2019), physiology and DT (Proctor et al., 2007; Coe et al., 2012), or exposure to differing environmental conditions (Reed et al., 2012). In particular, C balance has the potential to reveal the effects of environmental stress (e.g., desiccation stress) on poikilohydric plants. For example, intra-annual physiological receptivity to ambient hydrological conditions (acclimation) can prime poikilohydric organisms to respond in different ways to precipitation events (Schonbeck and Bewley, 1981; Hájek and Vicherová, 2014; Stark et al., 2014). However, responses of poikilohydric plant CO_2 exchange to hydration vs. desiccation acclimation, especially on timescales allowing growth for several months, have yet to be assessed. Capturing such variation using a framework such as C balance is important from ecophysiological as well as molecular perspectives related to desiccation and rehydration.

While C balance has been applied ad libitum in several environmental contexts (e.g., Reed et al., 2012; Coe et al., 2012, 2019) using custom-built benchtop instrumentation and incremental improvements in techniques, a

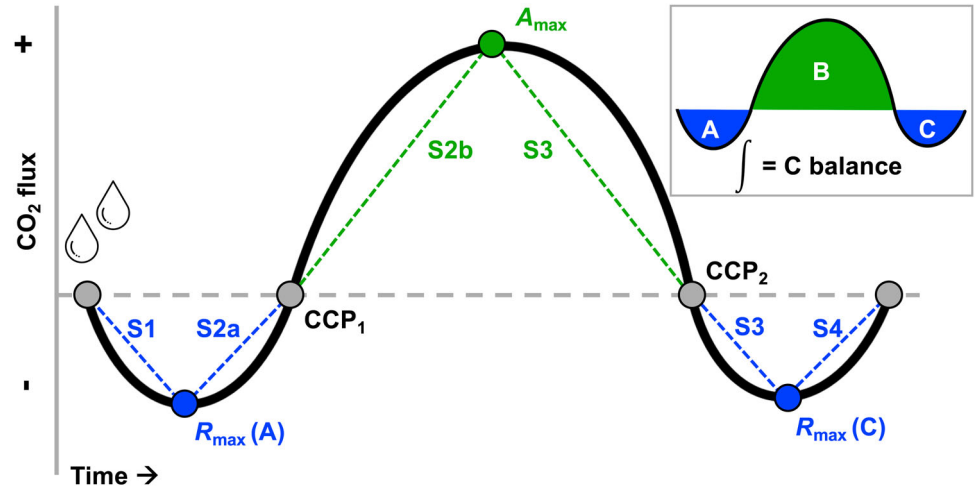

FIGURE 1 Representative C balance curve showing three characteristic phases of C flux during a dry–wet–dry cycle in a poikilohydric plant: initial respiration-dominated C loss phase (A), secondary photosynthesis-dominated phase of net C gains (B), and final respiration-dominated phase of C loss (C). The integrated area of the three phases represents the C balance for the hydration event (inset). Also shown are extractable values from each curve: the maximum net respiration rates during phases A (R_{max} [A]) and C (R_{max} [C]); the maximum net photosynthetic rate (A_{max}); and the slopes during the A phase (S1 and S2a), B phase (S2b and S3), and C phase (S3 and S4). Note that slope 2 has been divided into 2a and 2b based on observations that these two components of the curve often vary, whereas slope 3 is typically more consistent for the duration of the drying period. The gray points where the curve crosses the *x*-axis indicate, in order, the start of the curve, the first CO_2 compensation point (CCP_1), the second CO_2 compensation point (CCP_2), and the total time of the curve.

comprehensive methodological framework that can be applied across systems has yet to be described. Several limitations have hampered previous attempts at accurate infrared gas analysis (IRGA)–based C flux measurements for poikilohydric organisms. First, real-time IRGA-based measurements require accurate a priori estimates of the hydrated photosynthetic area to be measured as well as the amount of water to be added to samples to simulate a full turgor-inducing precipitation event. Second, many poikilohydric plants live in close association with their substrate, which must be considered during measurements. This is because removal from the substrate can damage plants or otherwise compromise plant structural integrity, and because microbial communities within substrates may also contribute to C fluxes during precipitation events. Finally, because initial physiological response to precipitation in poikilohydric plants can occur as early as seconds following water addition, capturing a complete C balance curve requires measurements immediately following hydration. A major limitation in previous studies measuring real-time C flux in poikilohydric organisms was that the IRGA measurement chamber required opening to hydrate dry samples followed by lengthy re-equilibration of internal conditions prior to measurement; we were able to solve this problem by implementing custom chamber modifications and a syringe method to allow water delivery into a closed system.

In this study, we present C balance as a tool for comparative assessments of photosynthetic physiology in poikilohydric plants, using the desiccation-tolerant dryland moss *S. caninervis* as a model system. Our goals were to (1) apply the C balance technique to mosses to examine ecophysiological variability in response to precipitation, (2) illustrate the flexibility of the C balance technique across a range of moisture conditions, (3) examine the ability of the C balance technique to distinguish between plants subjected to different hydration acclimation conditions (field collected vs. lab cultivated), and (4) produce an R Markdown product for application of the technique across plant systems. Along with C balance curves, which provide concise visual and numerical depictions of differential dynamics of C fluxes at the organismal scale, we also present 19 extracted variables from each C balance that can serve as comparative analytical metrics among samples.

METHODS AND RESULTS

Standard curve construction

Prior to C balance sample analysis, we developed standard curves to use the dry surface area of a sample (SA_{dry}) to predict its photosynthetic area once hydrated (SA_{wet}; EQ. 1; Figure A1), the volume of water needed to saturate an associated substrate (V_s; EQ. 2; Figure A2), and the volume of water needed for the plant to reach full turgor given a saturated substrate (V_p; EQ. 3; Figure A3). Each curve was created using 24–27 previously collected populations of *S. caninervis*. A detailed protocol for preparing the standard curves can be found in Appendix 1. The variables measured in each of the standard curves exhibited linear relationships; therefore, we applied linear models to create equations for SA_{wet}, V_s, and V_p. The equations generated from the standard curves were as follows:

$$SA_{wet} = 1.2374 \times SA_{dry} + 7.367 \quad (1)$$

$$V_s = (0.0156 \times \text{soil dry mass}) + 0.4169 \quad (2)$$

$$V_p = (0.0032 \times SA_{dry} - 0.84) + V_s \quad (3)$$

Sample preparation

The C balance procedure requires samples to be desiccated to begin measurement of C flux during a dry–wet–dry cycle. Samples that were not already dry (e.g., hydration-acclimated, lab-cultivated samples) were desiccated for 48 h using desiccation chambers set to produce headspaces of 38% ± 5% relative humidity (RH) at 21°C ± 0.7°C. Immediately prior to measurement, dry samples were removed from the desiccation chambers and placed in 35-mm Petri dishes. Previously desiccated samples (e.g., field-desiccated) were instead placed immediately in Petri dishes. The samples were approximately 30 mm in diameter; if samples were smaller or had separated during storage, then multiple pieces of moss sample were placed together to form a cushion ~30 mm in diameter. Samples were then analyzed for SA_{dry}, and standard curves were applied to estimate SA_{wet}, V_s, and V_p.

Infrared gas analysis

Carbon flux measurements were conducted over the course of a dry–wet–dry cycle using a LI-6800 infrared gas analyzer (LI-COR Biosciences, Lincoln, Nebraska, USA). The C balance procedure applies several important modifications to the standard instrument setup (Figure 2). First, as C balance curves can require constant data collection for 12 h or longer, use and regular replacement of the individual CO_2 canisters (typically lasting 4–8 h depending on CO_2 delivery rates) would interrupt data collection. To resolve this issue, we modified the setup to include in-line delivery of CO_2 from an external 50-lb cylinder to the CO_2 port in the LI-6800 control unit. Second, as assessment of C fluxes from poikilohydric organisms requires the ability to capture C dynamics within seconds of hydration, it is important that the measurement chamber not be opened for sample hydration. This is because it can take several minutes for the internal conditions within the chamber to restabilize once closed, and accurate measurements are only possible once conditions are stable. To solve this issue, we created a within-chamber hydration system including a syringe-sprayer to deliver water to the plant within the closed measurement system (Figure 2). This included a custom 3D-printed baseplate for the LI-6800-24 small plant/

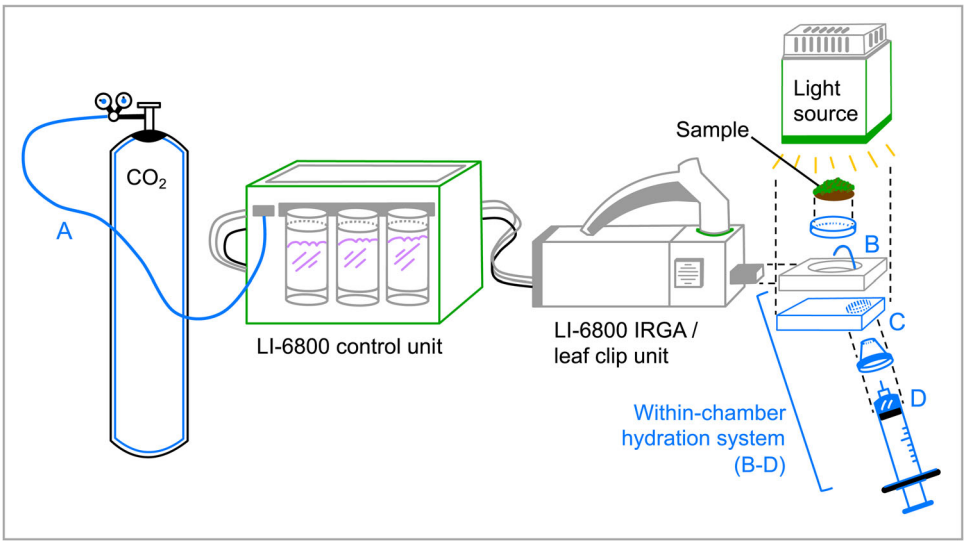

FIGURE 2 Diagram of setup for collecting data for C balance curves. Innovations and modifications are shown in blue and denoted by the letters A–D, and sections of the instrumentation expanded for ease of viewing are shown with dashed line connectors. A LI-6800 (LI-COR Biosciences) was used as the baseline instrument, including the LI-6800 large light source (6800-03) and the upper portion of the bryophyte chamber (6800-24). We modified the setup to include constant delivery of CO_2 via an attached external cylinder (A), a within-chamber hydration system including a syringe-sprayer to deliver water into the closed system (B), a custom 3D-printed chamber baseplate containing a cylindrical cutout for the silicone plug (C), and a syringe-based delivery system (D). Diagram is not to scale.

bryophyte chamber containing a cylindrical cutout for a silicone plug and a syringe-based delivery system that inserted into the plug (Appendices S1, S2; see Supporting Information with this article). This enabled us to deliver a predetermined amount of water (V_p) to the specimen within the chamber while C flux measurements were being taken.

Finally, to account for close interactions between poikilohydric plants and their substrates and for soil microbial activity that may influence C fluxes, we ran a three-step data collection process to isolate the plant C signal and produce a plant C balance curve. This included an initial plant+substrate curve, a substrate-only curve (for a description of how substrate-only curves were generated, see Appendix 1), and an analytical procedure to separate the plant signal from that of the substrate.

Data processing, visualization, and analysis

All data were viewed and analyzed using the open-source platform R (R Core Team, 2022). An annotated R Markdown (RMD) file detailing data manipulation and analyses is provided in Appendix S3. Raw data from the LI-6800 from each curve were loaded into this R script for all subsequent analyses.

To generate C balance curves for plant samples, the plant+substrate and the substrate-only data were first processed separately, then combined into a composite (plant-isolated) C balance curve. The data from each curve were trimmed to the end time of the respective curves in order to remove additional unnecessary data points (typically zeroes) collected following complete desiccation of samples. The two curves were then combined to create a composite curve that reflects the plant C balance for the precipitation event. This was accomplished by subtracting the substrate-only curve C assimilation values from the plant+substrate curve assimilation values. Following the construction of each C balance curve, 19 different parameters were extracted from the curve (Table 1, Figure 1).

Hydration stress case study: Sample collection and treatments

Samples of *S. caninervis* were collected in October and November 2018 from the Sheep Mountain range in southern Nevada, USA, within the Desert National Wildlife Refuge from a mid-elevation vegetation zone (1680 m, 36.51723 N, 115.16191 W) dominated by blackbrush (*Coleogyne ramosissima* Torr.), Joshua tree (*Yucca brevifolia* Engelm.), Mormon tea (*Ephedra viridis* Coville), and soil biocrust communities. For additional information on site environmental characteristics, see Clark (2020). All samples were collected >1 m apart and were growing in distinct patches; therefore, following accepted practice for discontinuously growing bryophytes, we refer to each collected sample as a separate population. Samples were collected dry and transported in a desiccated state to the laboratory at Middlebury College (Vermont, USA).

Each field-collected sample population was replicated in the lab environment for comparison, creating two treatment categories: desiccation-acclimated (field-collected) phenotype ($n = 5$) and hydration-acclimated (lab-cultivated) phenotype ($n = 5$). Samples in the desiccation-acclimated treatment were

TABLE 1 Comparison of extracted variables from C balance curves from desiccation-acclimated ($n = 5$) and hydration-acclimated ($n = 5$) populations of *Syntrichia caninervis*. Total C balance and areas of phases A, B, and C were calculated on an area basis using integrals between places where the curve crossed zero.[a]

Variable	Unit	Hydration-acclimated phenotype	Desiccation-acclimated phenotype	*t* value	*P* value[b]
Total C balance	$\mu mol \cdot m^{-2}$	13.94 ± 3.43	−2.45 ± 1.02	−4.32	0.012*
CCP_1	minutes	13.40 ± 2.502	192.2 ± 12.77	16.07	<0.0001***
CCP_2	minutes	409.0 ± 16.55	330.2 ± 52.43	−1.153	0.313
A phase area	$\mu mol \cdot m^{-2}$	−0.07 ± 0.03	−2.93 ± 0.68	−4.129	0.015*
Total dry time	minutes	516.8 ± 61.96	426.2 ± 61.43	−0.829	0.454
R_{max} (A)	$\mu mol \cdot m^{-2} \cdot s^{-1}$	−0.977 ± 0.458	−3.469 ± 1.019	−2.118	0.102
Time to R_{max} (A)	minutes	3.400 ± 0.872	36.40 ± 11.31	2.851	0.046*
A_{max}	$\mu mol \cdot m^{-2} \cdot s^{-1}$	6.423 ± 1.383	1.114 ± 0.111	−3.886	0.018*
B phase area	$\mu mol \cdot m^{-2}$	14.35 ± 3.670	0.88 ± 0.38	−3.596	0.022*
Time to A_{max}	minutes	129.16 ± 33.85	286.8 ± 45.43	2.858	0.046*
R_{max} (C)	$\mu mol \cdot m^{-2} \cdot s^{-1}$	−0.220 ± 0.129	−0.556 ± 0.200	−1.737	0.157
Time to R_{max} (C)	minutes	465.0 ± 47.24	361.8 ± 53.30	−1.111	0.329
C phase area	$\mu mol \cdot m^{-2}$	−0.35 ± 0.26	−0.40 ± 0.18	−0.152	0.887
Slope 1	$\mu mol \cdot m^{-2} \cdot s^{-2}$	−0.453 ± 0.243	−0.190 ± 0.097	0.896	0.421
Slope 2a	$\mu mol \cdot m^{-2} \cdot s^{-2}$	0.096 ± 0.047	0.023 ± 0.007	−1.671	0.17
Slope 2b	$\mu mol \cdot m^{-2} \cdot s^{-2}$	0.044 ± 0.008	0.017 ± 0.003	−2.982	0.041*
Slope 2	$\mu mol \cdot m^{-2} \cdot s^{-2}$	0.047 ± 0.009	0.021 ± 0.006	−2.423	0.073
Slope 3	$\mu mol \cdot m^{-2} \cdot s^{-2}$	−0.012 ± 0.009	−0.023 ± 0.003	−0.136	0.245
Slope 4	$\mu mol \cdot m^{-2} \cdot s^{-2}$	0.004 ± 0.001	0.009 ± 0.004	1.55	0.196

Note: CCP = CO_2 compensation point; R_{max} = maximum rate of net negative CO_2 exchange during respiratory phases A and C; A_{max} = maximum light-saturated net positive CO_2 exchange during photosynthetic phase B.

[a]See Figure 1 for curve locations of extracted variables including slopes 1–4 (S1–S4).

[b]$^*P < 0.05$, $^{***}P < 0.0001$.

left undisturbed in coin envelopes until preparation for measurement. To grow samples for the hydration-acclimated treatment, 5–7 shoots from each field-collected sample were removed and placed in a 35-mm Petri dish containing sterile sand growth media (collected from Utah, USA, and autoclaved at facilities at Middlebury College). Hydration-acclimated samples were allowed to grow to a predetermined adult/mature stage, possessing at least three whorls of leaves or 12 leaves total (Coe et al., 2021). Sample growth took place within a Percival E-30B growth chamber (Percival Scientific, Perry, Iowa, USA) maintained at 70% ± 10% RH, a 12-h day–night cycle with temperatures of 20°C and 8°C, respectively, and 25–55 μmol light intensity during day periods (Stark, 2017). With the exception of light levels, which were kept intentionally lower during shoot maturation, these settings closely matched the temperature, humidity, and day length conditions of the collection site between the months of September and December, when samples were collected from the Mojave Desert. Moss subcultures were hydrated biweekly to reach or just exceed full turgor, as previously determined to optimize growth in hydration-acclimated conditions (Stark, 2017). Hydration was achieved by alternating autoclaved deionized water with Hoagland's solution diluted to ~30% strength containing the macronutrients $Ca(NO_3)_2 \cdot 4H_2O$, KNO_3, $MgSO_4 \cdot 7H_2O$, and KH_2PO_4. All watering solutions also contained 50 $mg \cdot L^{-1}$ concentration of the antibiotic vancomycin, which we had previously determined to reduce contamination by fungi and other microbes during culturing without harming moss (determined using F_v/F_m [maximum quantum yield of photosystem II] recordings in moss grown with or without vancomycin).

We conducted complete C balance curves for each moss sample. To analyze differences in C balance and the 19 parameters extracted from each C balance curve measured on desiccation-acclimated and hydration-acclimated groups, data were assessed for normality and homoscedasticity, then Welch's *t*-tests (paired when appropriate) were performed to test for differences in means between the groups using $\alpha = 0.05$.

Carbon balance based on hydration conditions

Carbon balance estimates differed substantially between mosses subjected to the different hydration acclimation treatments (desiccation acclimated vs. hydration acclimated) in terms of plant+substrate and substrate-only component C flux curves (Figure 3), replicate net C balance curves measured on populations subjected to different hydration pre-conditions (Figure 4), and an array of extracted curve variables compared across treatments (Table 1).

In the hydration-acclimated phenotype, the C balance curve for the plant+substrate consisted of a distinct B phase of C gain from the atmosphere (positive numbers; Figure 3A), and minimal C losses (negative numbers) at the onset of hydration (phase A) and at the end of the curve (phase C). Carbon gains from the plant+substrate were greatest during the hydrated, photosynthetic phase (phase B), where positive net CO_2 exchange reached ~4 $\mu mol \cdot m^{-2} \cdot s^{-1}$. The substrate from the hydration-acclimated phenotype exhibited a gradual release of C to the atmosphere lasting ~5.5 h that peaked just under 4 h following hydration, which was approximately the same time as maximum C fixation in the moss. The resulting net C balance of the moss was 12.20 $\mu mol \cdot m^{-2}$ for the entire hydration event, during which the moss required ~8 h to dry completely. The maximum rate of net C fixation (A_{max}) was 5.68 $\mu mol \cdot m^{-2} \cdot s^{-1}$ and occurred 3.8 h after rehydration. The maximum respiration rate was −0.33 $\mu mol \cdot m^{-2} \cdot s^{-1}$ and the initial CO_2 compensation point was reached 15 min after rehydration.

In the desiccation-acclimated phenotype (Figure 3B), the plant+substrate and plant-only C balance curves both exhibited distinct A, B, and C phases. Carbon fluxes observed in the substrate-only curve were minimal ($R_{max} \sim -1.0$ $\mu mol \cdot m^{-2} \cdot s^{-1}$) and occurred mainly in the first 2 h after rehydration. The resulting net C balance curve displayed a large A phase, where respiration peaked at −4.08 $\mu mol \cdot m^{-2} \cdot s^{-1}$ 18 min after hydration. The initial CO_2 compensation point in the desiccation-acclimated plant was reached 3.41 h following hydration. Subsequently, a small B phase was observed, where A_{max} reached 1.12 $\mu mol \cdot m^{-2} \cdot s^{-1}$, and a significant C phase was observed, where the maximum respiration reached −1.12 $\mu mol \cdot m^{-2} \cdot s^{-1}$ 5.5 h after hydration. The resulting net C balance for the desiccation-acclimated sample was −4.57 $\mu mol \cdot m^{-2}$ following the precipitation event.

In replicate curves measured on the populations exhibiting either the desiccation-acclimated phenotype or hydration-acclimated phenotype, net C balance curves were distinct in several key ways (Figure 4, Table 1). Notably, the

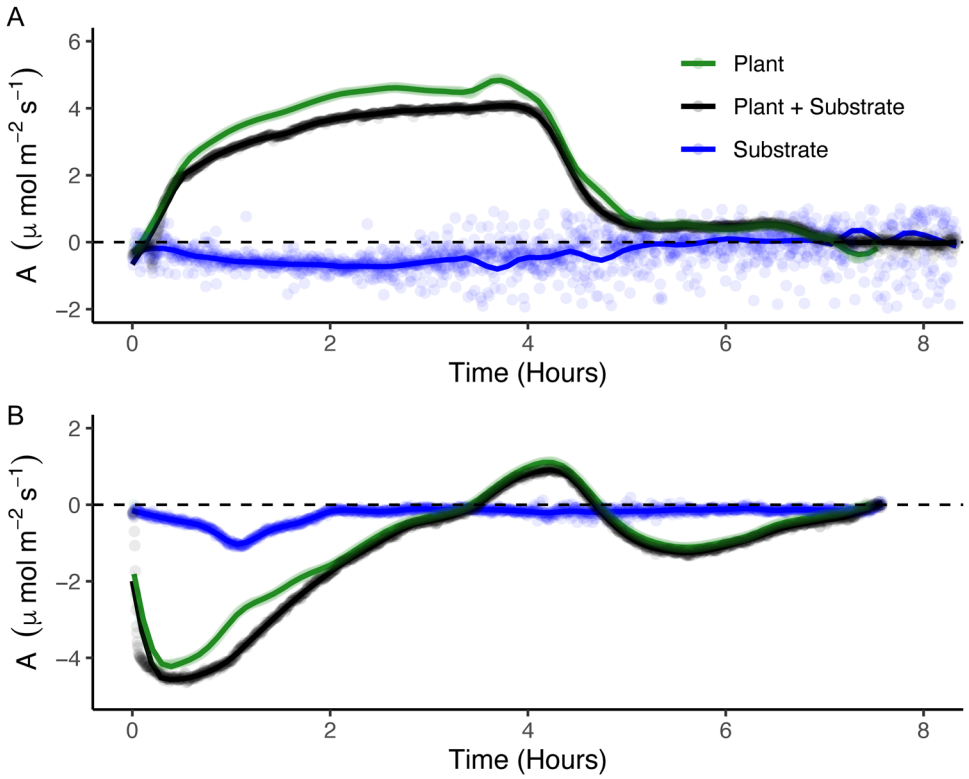

FIGURE 3 Representative C balance curves, and the three-step data collection process to create them, for samples of the same moss population exhibiting the hydration-acclimated (lab-cultivated) phenotype (panel A) or desiccation-acclimated (field-collected) phenotype (panel B). Each panel shows C flux (A, $\mu mol \cdot m^{-2} \cdot s^{-1}$) as a function of time since hydration (occurring once at t = 0 h in each case). The black line shows the carbon flux of the initial plant+substrate IRGA run, the blue line shows the substrate-only curve, and the green line represents the substrate-only curve subtracted from the plant+substrate curve, isolating the plant-associated C balance curve. Lines are local regression models with a span of 0.1 (this value best illustrates biologically relevant curve microdynamics) made up of A values taken every 15 s, and points shown are original data points collected during IRGA from which local regression models were generated.

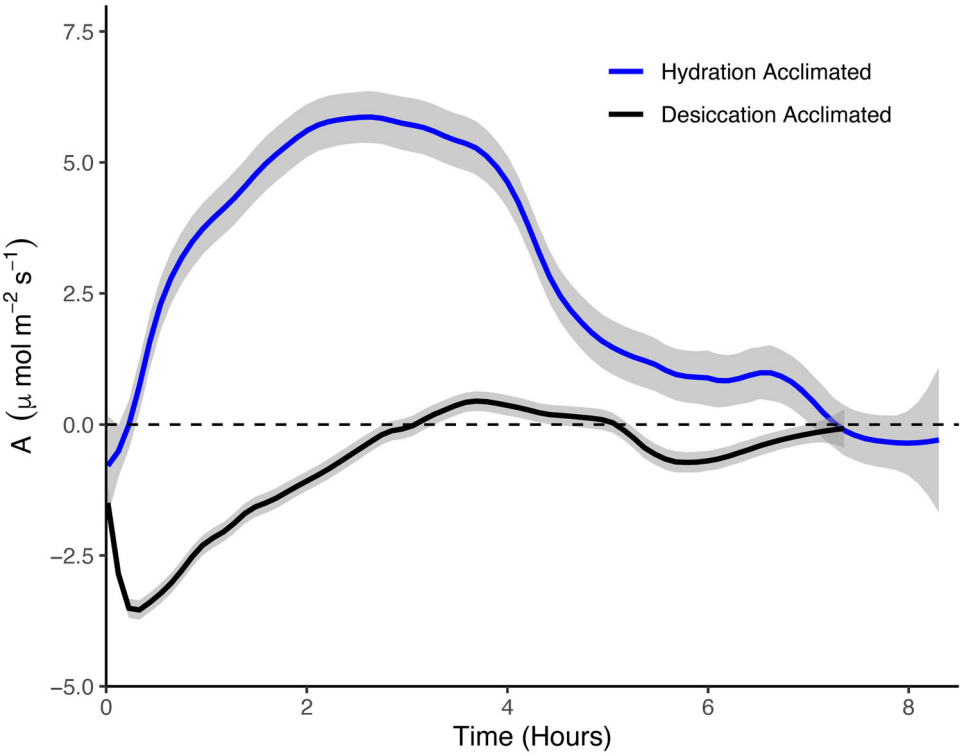

FIGURE 4 Comparison of net C balance curves measured on populations of *Syntrichia caninervis* subjected to desiccation-acclimated (field-collected, black; lower curve) or hydration-acclimated (lab-cultivated, blue; upper curve) conditions. In each curve, C flux (A, μmol·m^{-2}·s^{-1}) is shown as a function of time since hydration; values above zero on the *y*-axis represent net C fluxes to the moss, and values below zero represent C fluxes to the air. Lines are local regressions with a span of 0.1 (this value best illustrates biologically relevant curve microdynamics) with $n = 5$ for each treatment. Gray-shaded bounds represent 95% confidence intervals for each local regression line.

average C balance was positive in the hydration-acclimated phenotype (13.94 ± 3.43 μmol·m^{-2}) and negative in the desiccation-acclimated phenotype (−2.45 ± 1.02 μmol·m^{-2}; $t = -4.32$, $P = 0.01$). Additional differences in the shapes of curves and resulting curve parameters were also captured. First, the integrated area of the initial respiratory (A) phase (i.e., the C loss at the onset of hydration) was an order of magnitude greater in the desiccation-acclimated phenotype (−2.93 ± 0.68 μmol·m^{-2}) compared to the hydration-acclimated phenotype (−0.07 ± 0.03 μmol·m^{-2}; $t = -4.32$, $P = 0.02$), and the initial CO_2 compensation point (CCP_1) was reached after 13.40 ± 2.50 min in the hydration-acclimated phenotype compared to 192.2 ± 12.77 min (~3.2 h) in the desiccation-acclimated phenotype ($t = 16.07$, $P < 0.0001$). The integrated area of the phase of net photosynthetic C gains (phase B) was also an order of magnitude greater in the hydration-acclimated phenotype (14.35 ± 3.67 μmol·m^{-2}) compared to the desiccation-acclimated phenotype (0.88 ± 0.38 μmol·m^{-2}; $t = -3.60$, $P = 0.02$). The hydration-acclimated phenotype exhibited a significantly higher A_{max} (6.42 ± 1.38 μmol·m^{-2}·s^{-1}) compared to the desiccation-acclimated phenotype (1.11 ± 0.11 μmol·m^{-2}·s^{-1}; $t = -3.89$, $P = 0.02$), which was also reached 2.6 h earlier ($t = 2.86$, $P = 0.04$). When comparing the six different slope elements of the curve, we found that slope 2b (the portion of the curve between CCP_1 and A_{max}) was significantly steeper in the hydration-acclimated compared to the desiccation-acclimated phenotype (0.04 ± 0.01 vs. 0.02 ± 0.003 μmol·m^{-2}·s^{-2}; $t = -2.98$, $P = 0.04$; Figure 4, Table 1).

CONCLUSIONS

Here we present the first complete C balance protocol and test its applicability on field-collected poikilohydric plants. By implementing methodological innovations to adapt IRGA-based measurements to the poikilohydric condition, then applying the C balance technique to desiccation-acclimated and hydration-acclimated phenotypes of field-collected plant populations, we were able to examine ecophysiological variability in response to precipitation, illustrate the flexibility of the C balance tool across moisture conditions and plant and substrate samples, and distinguish between populations subjected to different environmental pretreatment conditions.

Implications of methodological innovations

Applying a method for continuous CO_2 delivery during IRGA enabled us to capture natural variation in dry–wet–dry cycle

length related to sample size and hydration amount. Additionally, implementation of a within-chamber hydration technique allowed us to measure real-time, biologically relevant C flux dynamics that occur immediately upon rehydration, substantially improving upon previous C flux data collection during plant dry–wet–dry cycles that required opening of the chamber to hydrate specimens (e.g., Coe et al., 2012). As has been previously shown (Coe et al., 2012; Reed et al., 2012) and as we have demonstrated here, poikilohydric plants can exhibit an extremely rapid burst of respiration immediately following hydration and reach the initial CO_2 compensation point (a critical threshold above which C fluxes become positive to the plant) shortly thereafter.

An additional methodological step we implemented was a three-phase curve creation protocol (Appendix 1, Figure 3) that included CO_2 flux measurements from the substrate on which plants were growing in addition to those from the plant itself. This is extremely important for cryptogams such as bryophytes or lichens, as well as for other plants that may either live in intimate contact with a substrate, for which removal from the substrate may induce damage to the plant or colony, and/or for which the growth substrate may also harbor C fixing or respiring microbiota. From this protocol we were able to produce reliable curves for plant+substrate and the substrate alone, then combine them to produce an accurate representation of isolated plant net C balance. In addition to effectively separating C fluxes from substrate and plant, this technique also enables direct measurement and comparison of substrate microbiota C fluxes in response to moisture. However, one current limitation of our three-step curve protocol is that the substrate is hydrated and desiccated two times, and pre-processing prior to running the substrate-only curve may modify the substrate texture or other biophysical features. This leaves open the potential for the substrate to respond differently between the initial plant+substrate curve and the substrate-only curve, especially in samples that had previously experienced extended droughts in the field.

Finally, complete data analysis of C flux data of this magnitude required a dedicated script file, and we created a flexible, annotated R Markdown source file applicable across watering regimes, pretreatments, and populations (see Appendix S3). This file includes an automated data cleaning and trimming procedure for both the plant+substrate and substrate-only curves, a sequential data visualization and figure development protocol, and a section of code to calculate and extract the 19 supplemental physiological parameters from each C balance curve. This R Markdown file is designed to be implemented broadly and applied across poikilohydric plant systems of interest (see "Applications to other poikilohydric organisms," below).

Comparison of C balance curves based on hydration pretreatment

Using the C balance technique, we were able to distinguish between moss populations of the same species subjected to different hydration pretreatment conditions. Specifically, we found that, when dried and rehydrated under otherwise identical conditions, mosses that underwent the hydration-acclimated treatment exhibited C gains following the simulated precipitation event, whereas those from the desiccation-acclimated treatment exhibited C losses. Large, sometimes order-of-magnitude differences based on hydration treatments were apparent in an array of extracted parameters from the C balance curves as well as in the shape of the curves themselves. The most notable of these differences were (1) large respiratory losses at the onset of hydration in the desiccation-acclimated phenotype compared to minimal C losses at this stage in the hydration-acclimated phenotype, (2) a 14-fold increase in the time to initial CO_2 compensation point, on average, in the desiccation-acclimated samples, and (3) an overall negative C balance in the desiccation-acclimated phenotype compared to the hydration-acclimated phenotype. In addition to plant CO_2 exchange differing across treatments, we also observed differences in CO_2 fluxes of the substrate (e.g., Figure 3), where substrates in the hydration-acclimated samples often exhibited a greater overall magnitude of C flux to the atmosphere than those from the desiccation-acclimated samples.

These findings illustrate the capacity of the C balance technique to capture dramatically differing responses to similar hydration levels (full turgor in all cases) based on previous exposure to moist or dry environments and are consistent with previous work suggesting the length of the dry interval prior to moisture is negatively correlated with C balance (Coe et al., 2012). The desiccation-acclimated samples were likely dry for at least several months (based on timing of field collection) prior to hydration, while the hydration-acclimated samples were dry for just 48 h prior to the simulated precipitation event. Based on the field conditions of the Nevada collection site, where average maximum RH was 39% ± 22% (Clark, 2020), desiccation-acclimated samples may also have experienced higher-intensity desiccation in the field compared to the hydration-acclimated samples. Our results therefore lend support to the existing hypothesis that there is an increased respiratory cost of rehydration following lengthy or more intense periods of desiccation in poikilohydric organisms (Hinshiri and Proctor, 1971; Green et al., 2011; Coe et al., 2012; Stark, 2017), and further suggest that, compared to the hydration-acclimated mosses, desiccation-acclimated mosses may have exhibited physiological stress upon this initial rehydration.

These results also illustrate the flexibility of the C balance technique to simulate different precipitation event sizes using the in-chamber hydration delivery system. As each of the five populations, whether grown in the wet condition or kept in the dry condition, had a different SA_{dry} (ranging from 297–997 mm^2), our standard curves for determining SA_{wet} as well as hydration level to reach full turgor (V_p) were each different for each sample within each treatment category.

Applications to other poikilohydric organisms

The C balance technique we present here can be applied across poikilohydric organisms, such as angiosperm resurrection plants, lichens, other bryophytes, or soil biocrust communities. Indeed, others have used earlier iterations of the C balance technique to determine C flux rates from poikilohydric plants growing on rock outcrops (Alpert and Oechel, 1985) and dryland biocrusts that include cyanobacteria, lichens, mosses, fungi, and other microorganisms (Grote et al., 2010). Our goal here was to contribute a standard protocol for widespread future use among investigators examining photosynthesis in poikilohydric plants. The C balance technique is extremely flexible, and, focusing here on applications to other poikilohydric autotrophs, we propose the following key points to consider for future investigations.

First, accurate CO_2 flux estimates for C balance curves require creation of functional group-specific standard curves to provide a priori estimates of SA_{wet}, V_p, and if required, V_s. This is because different poikilohydric plant groups are likely to exhibit differing relationships to hydration and responses during desiccation. This can be accomplished by applying our standard curve protocols to capture the relevant range of variation in SA_{dry} in the target plant functional group. Additionally, for some biocrust taxa that possess more intimate substrate relationships, separation of the substrate–C signal may require modified protocols.

Second, analytical processing steps following data collection will require application and potential modification of the R Markdown protocols described here based on the physiological characteristics of the plants of interest. This may include modifications to the curve cleaning protocol based on known responses to water addition, such as differing rates of desiccation or expected length of time hydrated, or modifications to substrate-only curve processing steps depending on substrate material and expected substrate response to hydration.

Finally, while in this paper we outline baseline protocols for measurement of full turgor-inducing hydration, it is simple and straightforward to test hypotheses related to global change–relevant hydrological stressors, such as drought, rapid desiccation, partial hydration, or oversaturation, by modification of one to several elements of the hydration and measurement protocols. Overall, we expect the C balance technique outlined here to be a critical resource for examining comparative photosynthetic physiology in poikilohydric plants, especially in a changing environment.

AUTHOR CONTRIBUTIONS

K.K.C. designed the overall C balance protocol; established innovations and modifications to the technique; designed the case study; mentored students performing the research, data collection, and interpretation; outlined the initial manuscript; and wrote the final manuscript with N.C.J. N.N. collected data for the case study presented in the manuscript, created the initial version of the RMD file for data processing, and contributed to manuscript revisions. M.I.G. contributed to modifications of the C balance technique, creation of standard curves, and development of initial R scripts for data processing, parameter extraction, and visualization. N.C.J. established standard curves used for data collection, participated in data analysis and figure creation for the manuscript, contributed to RMD script revisions, and wrote the final version of the manuscript with K.K.C. All authors approved the final version of the manuscript.

ACKNOWLEDGMENTS

The authors thank the sources of funding for this research, including the National Science Foundation Dimensions of Biodiversity Program (award no. 1840931 to K.K.C.), the Middlebury College Biology Department, and the Middlebury Senior Research Project Supplement Fund. We also wish to thank Theresa Clark (University of Nevada Las Vegas) for careful field collection of specimens, Llo Stark (University of Nevada Las Vegas) for stimulating intellectual conversations about the C balance technique and a friendly review of this manuscript, Josh Greenwood (University of Nevada Las Vegas) for the initial development of the 3D code of the chamber base used in data collection, Sahalie Pittman (Middlebury College) for data collection and contributions to standard curve development, and finally Brent Mishler (University of California Berkeley), Mel Oliver (University of Missouri), Steve Rice (Union College), and Nancy Slack (Russell Sage College) for discussions about the C balance technique over the past 10 years.

DATA AVAILABILITY STATEMENT

A detailed carbon balance protocol, RMD file, custom chamber baseplate data files, and standard curve data are available in the Supporting Information for this manuscript. All other data used in the manuscript, including in the hydration-acclimation case study, are available via the public GitHub repository (https://github.com/KirstenKCoe/Coe-et-al.-2024-APPS).

ORCID

Kirsten K. Coe http://orcid.org/0000-0002-1560-8022
Maya I. Gomez http://orcid.org/0000-0003-2194-7140
Niko Carvajal Janke http://orcid.org/0000-0002-6059-5785

REFERENCES

Alpert, P., and W. C. Oechel. 1985. Carbon balance limits the microdistribution of *Grimmia laevigata*, a desiccation-tolerant plant. *Ecology* 66(3): 660–669.

Asami, P., T. Rupasinghe, L. Moghaddam, I. Njaci, U. Roessner, S. Mundree, and B. Williams. 2019. Roots of the resurrection plant *Tripogon loliiformis* survive desiccation without the activation of autophagy pathways by maintaining energy reserves. *Frontiers in Plant Science* 10: 459.

Bewley, J. D. 1979. Physiological aspects of desiccation tolerance. *Annual Review of Plant Physiology* 30(1): 195–238.

Bota, J., H. Medrano, and J. Flexas. 2004. Is photosynthesis limited by decreased Rubisco activity and RuBP content under progressive water stress? *New Phytologist* 162(3): 671–681.

Clark, T. A. 2020. Can desert mosses hide from climate change? The ecophysiological importance of habitat buffering and water relations to a keystone biocrust moss in the Mojave Desert. Ph.D. dissertation, University of Nevada, Las Vegas, Nevada, USA.

Coe, K. K., and J. P. Sparks. 2014. Physiology-based prognostic modeling of the influence of changes in precipitation on a keystone dryland plant species. *Oecologia* 176: 933–942.

Coe, K. K., J. Belnap, and J. P. Sparks. 2012. Precipitation-driven carbon balance controls survivorship of desert biocrust mosses. *Ecology* 93(7): 1626–1636.

Coe, K. K., N. B. Howard, M. L. Slate, M. A. Bowker, B. D. Mishler, R. Butler, J. Greenwood, and L. R. Stark. 2019. Morphological and physiological traits in relation to carbon balance in a diverse clade of dryland mosses. *Plant, Cell & Environment* 42(11): 3140–3151.

Coe, K. K., J. L. Greenwood, M. L. Slate, T. A. Clark, J. C. Brinda, K. M. Fisher, B. D. Mishler, et al. 2021. Strategies of desiccation tolerance vary across life phases in the moss *Syntrichia caninervis*. *American Journal of Botany* 108(2): 249–262.

Flexas, J., J. Bota, J. Galmés, H. Medrano, and M. Ribas-Carbó. 2006. Keeping a positive carbon balance under adverse conditions: Responses of photosynthesis and respiration to water stress. *Physiologia Plantarum* 127(3): 343–352.

Green, T. A., L. G. Sancho, and A. Pintado. 2011. Ecophysiology of desiccation/rehydration cycles in mosses and lichens. *In* U. Lüttge, E. Beck, and D. Bartels [eds.], Plant desiccation tolerance, 89–120. Springer, Berlin, Germany.

Green, J. K., S. I. Seneviratne, A. M. Berg, K. L. Findell, S. Hagemann, D. M. Lawrence, and P. Gentine. 2019. Large influence of soil moisture on long-term terrestrial carbon uptake. *Nature* 565(7740): 476–479.

Grote, E. E., J. Belnap, D. C. Housman, and J. P. Sparks. 2010. Carbon exchange in biological soil crust communities under differential temperatures and soil water contents: Implications for global change. *Global Change Biology* 16(10): 2763–2774.

Hájek, T., and E. Vicherová. 2014. Desiccation tolerance of *Sphagnum* revisited: A puzzle resolved. *Plant Biology* 16(4): 765–773.

Hamerlynck, E. P., Z. Tuba, Z. Csintalan, Z. Nagy, G. Henebry, and D. Goodin. 2000. Diurnal variation in photochemical dynamics and surface reflectance of the desiccation-tolerant moss, *Tortula ruralis*. *Plant Ecology* 151(1): 55–63.

Hinshiri, H. M., and M. C. F. Proctor. 1971. The effect of desiccation on subsequent assimilation and respiration of the bryophytes *Anomodon viticulosus* and *Porella platyphylla*. *New Phytologist* 70(3): 527–538.

Jung, P., D. Emrich, L. Briegel-Williams, M. Schermer, L. Weber, K. Baumann, and B. Büdel. 2019. Ecophysiology and phylogeny of new terricolous and epiphytic chlorolichens in a fog oasis of the Atacama Desert. *MicrobiologyOpen* 8(10): e894.

Kondo, F., K. Ono, M. Mano, A. Miyata, and O. Tsukamoto. 2014. Experimental evaluation of water vapour cross-sensitivity for accurate eddy covariance measurement of CO_2 flux using open-path CO_2/H_2O gas analysers. *Tellus B: Chemical and Physical Meteorology* 66(1): 23803.

Lavorel, S., and É. Garnier. 2002. Predicting changes in community composition and ecosystem functioning from plant traits: Revisiting the Holy Grail. *Functional Ecology* 16(5): 545–556.

Lawlor, D. W. 2002. Limitation to photosynthesis in water-stressed leaves: Stomata vs. metabolism and the role of ATP. *Annals of Botany* 89(7): 871–885.

Lawson, T., and S. Vialet-Chabrand. 2019. Speedy stomata, photosynthesis and plant water use efficiency. *New Phytologist* 221(1): 93–98.

Mishler, B. D., and M. J. Oliver. 2009. Putting *Physcomitrella patens* on the tree of life: The evolution and ecology of mosses. *In* C. D. Knight, P.-F. Perroud, and D. J. Cove [eds.], The Moss *Physcomitrella patens*, 1–15. Annual Plant Reviews, 36. Wiley-Blackwell, Oxford, United Kingdom.

Moore, J. P., N. T. Le, W. F. Brandt, A. Driouich, and J. M. Farrant. 2009. Towards a systems-based understanding of plant desiccation tolerance. *Trends in Plant Science* 14(2): 110–117.

Oliver, M. J., S. E. Dowd, J. Zaragoza, S. A. Mauget, and P. R. Payton. 2004. The rehydration transcriptome of the desiccation-tolerant bryophyte *Tortula ruralis*: Transcript classification and analysis. *BMC Genomics* 5: 89.

Oliver, M. J., J. E. F. F. Velten, and B. D. Mishler. 2005. Desiccation tolerance in bryophytes: A reflection of the primitive strategy for plant survival in dehydrating habitats? *Integrative and Comparative Biology* 45(5): 788–799.

Proctor, M. C. 2004. How long must a desiccation-tolerant moss tolerate desiccation? Some results of 2 years' data logging on *Grimmia pulvinata*. *Physiologia Plantarum* 122(1): 21–27.

Proctor, M. C., and Z. Tuba. 2002. Poikilohydry and homoihydry: Antithesis or spectrum of possibilities? *New Phytologist* 156(3): 327–349.

Proctor, M. C., R. Ligrone, and J. G. Duckett. 2007. Desiccation tolerance in the moss *Polytrichum formosum*: Physiological and fine-structural changes during desiccation and recovery. *Annals of Botany* 99(1): 75–93.

R Core Team. 2022. R: A language and environment for statistical computing. R Foundation for Statistical Computing, Vienna, Austria. https://www.R-project.org/

Reed, S. C., K. K. Coe, J. P. Sparks, D. C. Housman, T. J. Zelikova, and J. Belnap. 2012. Changes to dryland rainfall result in rapid moss mortality and altered soil fertility. *Nature Climate Change* 2(10): 752–755.

Schneider, C. A., W. S. Rasband, and K. W. Eliceiri. 2012. NIH Image to ImageJ: 25 years of image analysis. *Nature Methods* 9(7): 671–675. https://doi.org/10.1038/nmeth.2089

Schonbeck, M. W., and J. D. Bewley. 1981. Responses of the moss *Tortula ruralis* to desiccation treatments. II. Variations in desiccation tolerance. *Canadian Journal of Botany* 59(12): 2707–2712.

Stanton, D. E., and K. K. Coe. 2021. 500 million years of charted territory: Functional ecological traits in bryophytes. *Bryophyte Diversity and Evolution* 43(1): 234–252.

Stark, L. 2005. Phenology of patch hydration, patch temperature and sexual reproductive output over a four-year period in the desert moss *Crossidium crassinerve*. *Journal of Bryology* 27: 231–240.

Stark, L. R. 2017. Ecology of desiccation tolerance in bryophytes: A conceptual framework and methodology. *The Bryologist* 120(2): 130–165.

Stark, L. R., J. L. Greenwood, J. C. Brinda, and M. J. Oliver. 2014. Physiological history may mask the inherent inducible desiccation tolerance strategy of the desert moss *Crossidium crassinerve*. *Plant Biology* 16(5): 935–946.

Tenhunen, J. D., A. S. Serra, P. C. Harley, R. L. Dougherty, and J. F. Reynolds, 1990. Factors influencing carbon fixation and water use by Mediterranean sclerophyll shrubs during summer drought. *Oecologia* 82: 381–393.

Tuba, Z., Z. Csintalan, and M. C. Proctor. 1996. Photosynthetic responses of a moss, *Tortula ruralis*, ssp. *ruralis*, and the lichens *Cladonia convoluta* and *C. furcata* to water deficit and short periods of desiccation, and their ecophysiological significance: A baseline study at present-day CO_2 concentration. *New Phytologist* 133(2): 353–361.

Tuba, Z., C. F. Protor, and Z. Csintalan. 1998. Ecophysiological responses of homoiochlorophyllous and poikilochlorophyllous desiccation tolerant plants: A comparison and an ecological perspective. *Plant Growth Regulation* 24: 211–217.

SUPPORTING INFORMATION

Additional supporting information can be found online in the Supporting Information section at the end of this article.

Appendix S1. Blender file containing the digital spatial information for 3D printing of the IRGA custom chamber baseplate.

Appendix S2. Image file showing the 3D structure of the custom chamber baseplate.

Appendix S3. An executable R file and associated annotations, providing a step-by-step guide to carbon balance data processing (following download from an IRGA such as a LI-6800), data visualization, three-phase curve construction and isolation of the plant signal, and extraction of physiological variables from each carbon balance curve for comparative analytics.

How to cite this article: Coe, K. K., N. Neumeister, M. I. Gomez, and N. C. Janke. 2024. Carbon balance: A technique to assess comparative photosynthetic physiology in poikilohydric plants. *Applications in Plant Sciences* 12(5): e11585. https://doi.org/10.1002/aps3.11585

Appendix 1. Materials list and carbon balance measurement protocol.

Materials list

Standard curve materials

Laminated 8.5 × 11 sheet of paper with one 4-cm^2 red square in the center
Syringe (10 mL)
Microbalance (e.g., Mettler Toledo XS105; Mettler Toledo, Columbus, Ohio, USA)
ImageJ Software
Dissecting binocular microscope
Small metric ruler (to measure in millimeters)
Sterile plastic Petri dishes (35 mm)

Desiccation protocol materials

Desiccation chambers (150 mL) (baby food jars work well)
Transparent lids for desiccation chambers
Salt for producing desired target relative humidity headspace (e.g., MgCl)
Hygrochron iButtons (Embedded Data Systems, Lawrenceburg, Kentucky, USA), one per desiccation chamber
Heavy pedestal (e.g., glass jar filled with BB pellets) that fits inside each desiccation chamber
Petri dishes (35 × 15 mm) (to act as a raised platform atop pedestal in which sample and iButton are placed during desiccation)

Infrared gas analysis materials

Modified LI-6800 Infrared Gas Analyzer (LI-COR Biosciences, Lincoln, Nebraska, USA) (see Figure 2)
Modified sample chamber baseplate with hole for silicone plug and syringe placement (see Appendices S1, S2)
Silicone plug with hole for syringe

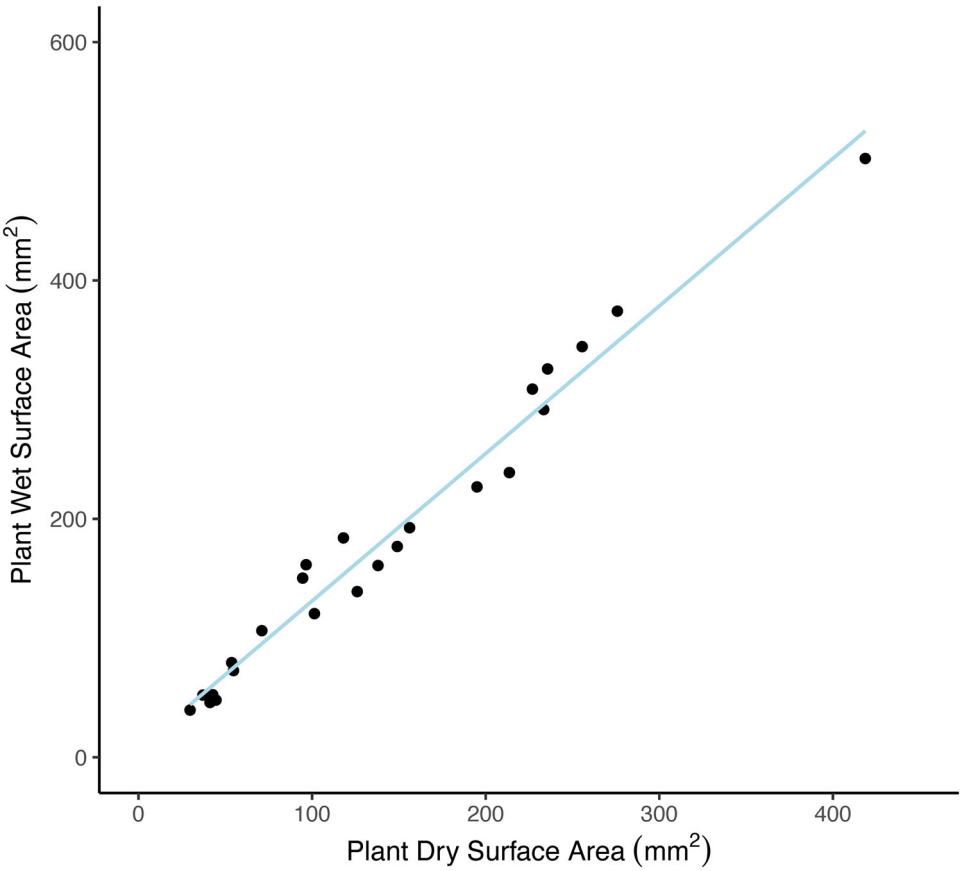

FIGURE A1 Linear model used to predict wet surface area (SA_{wet}) of *Syntrichia caninervis* samples at the beginning of each carbon balance curve using initial dry surface area (SA_{dry}). The trendline used the known parameters of 24 *Syntrichia caninervis* samples. $y = 1.2374 \times x + 7.367$, $R^2 = 0.9725$.

Syringe (size dependent on desired specimen hydration amount) with bendable needle tip
Large (e.g., 50 lb) CO_2 tank and regulator
CO_2 tank to LI-6800 adapter kit (part number 9968-109; LI-COR Biosciences) and copper tubing
Microbalance (e.g., Mettler Toledo XS105)

Carbon balance measurement protocol

Standard curve construction

We used standard curves to use the dry surface area of a sample (SA_{dry}) to predict its photosynthetic area once hydrated (SA_{wet}; EQ. 1; Figure A1), the volume of water required to be added to saturate the substrate (V_s; EQ. 2; Figure A2), and the volume of water needed for the plant to reach full turgor given a saturated substrate (V_p; EQ. 3; Figure A3).

To determine the relationship between SA_{dry} and SA_{wet}, measure the two-dimensional area (a_{dry}) of samples in the desiccated state from above, hydrate them to full turgor (following the protocols below), then measure their two-dimensional area again in the wet state (a_{wet}). First, photograph dry samples from a fixed height using a photo of a 4-cm^2 red square as a known measurement. Isolate the red channel of the image using ImageJ (Schneider et al., 2012), and use channel thresholding to record the sample area (mm^2) of the top of the moss tissue. Record the height (h) of the sample in millimeters as the average from three locations in the sample. SA_{dry} can then be calculated as the surface area of a cylinder without a base (as the base of the plant sample is not photosynthesizing) from the height and top surface area measurement of the sample, using the following equation.

$$SA = 2\pi\sqrt{\frac{a}{\pi}}(\mathrm{h}) + \pi\left(\sqrt{\frac{a}{\pi}}\right)^2$$

To determine the relationship between SA_{dry} and V_p, quantify the volume of water required to achieve full turgor for each sample. Under a dissecting microscope, add droplets of water of a known volume to the center of the desiccated moss sample, allowing time for the droplet to be absorbed into the tissue. Once a drop begins pooling on the moss leaves and is no longer absorbed into the tissue, subtract the volume of the last drop and consider that sample hydrated to full turgor. Record the volume of water needed to hydrate that sample as V_p. Hydrated moss samples can then be photographed, processed through

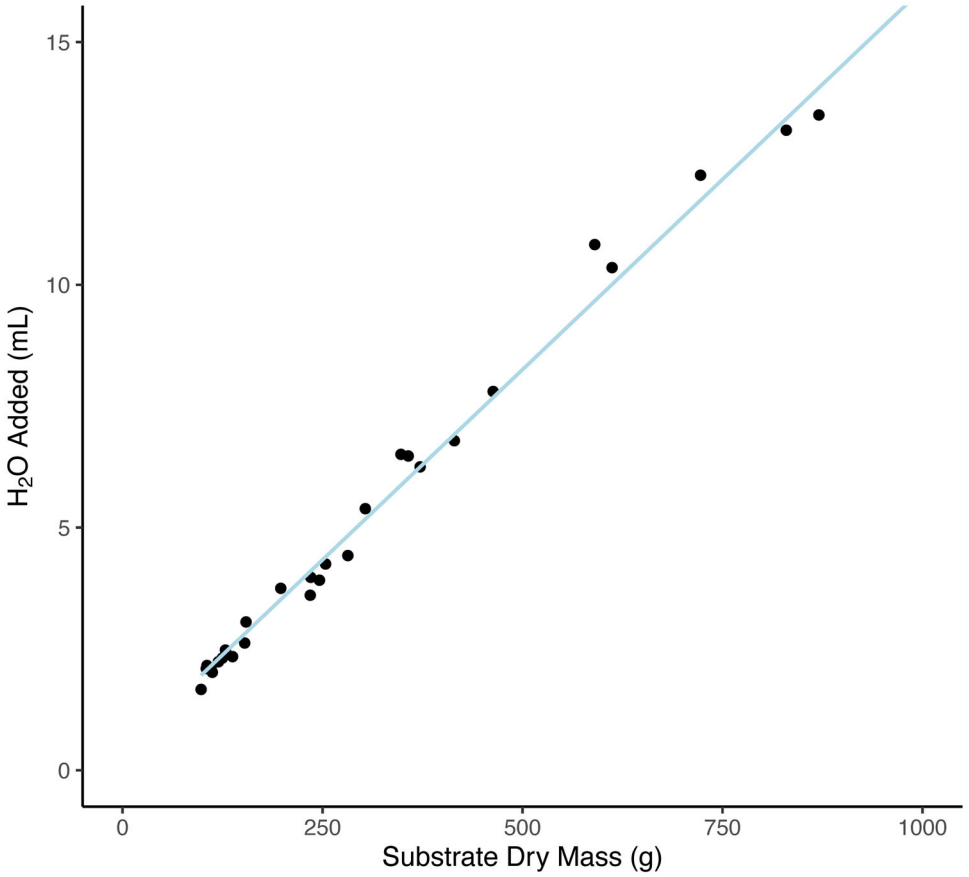

FIGURE A2 Linear model used to calculate the amount of water needed to hydrate the substrate (V_s) of *Syntrichia caninervis* samples at the beginning of each carbon balance curve using its initial dry mass. The trendline used the known parameters of 27 *Syntrichia caninervis* samples. $y = (0.0156 \times x) + 0.4169$, $R^2 = 0.9915$.

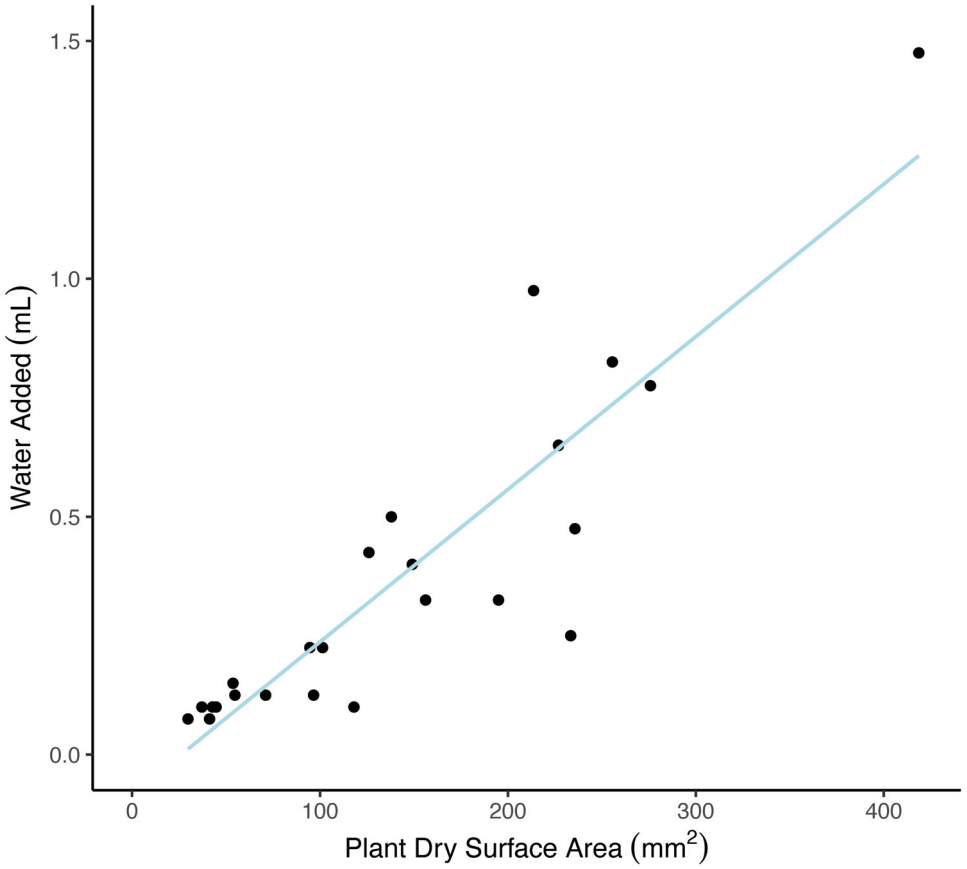

FIGURE A3 Linear model used to predict the volume of water added (V_p) to *Syntrichia caninervis* plant samples at the beginning of each carbon balance curve using its initial dry surface area (SA_{dry}). The trendline used the known parameters of 24 *Syntrichia caninervis* samples. $y = (0.0032 \times x - 0.84)$, $R^2 = 0.7931$.

ImageJ red channel thresholding as described above, and measured for height following the same protocol as the desiccated samples to generate SA_{wet}. The photosynthetic surface area method applied here is based on previous work in which a uniform height of green, photosynthetic tissue was observed on the adaxial cushion surface in *Syntrichia caninervis* (Coe et al., 2012).

To determine V_s, the amount of water to be added to the substrate, create a standard curve for substrate saturation using a relevant range of substrate amounts. For each substrate sample, measure the dry mass using an analytical balance (we used the Mettler Toledo XS105), then add water one drop at a time as described above until the substrate is fully saturated. Full saturation is determined under a dissecting scope based on the presence of a fine water film appearing on the substrate surface. When this is observed, the volume of one drop should be subtracted from the total to determine the saturating water volume (i.e., field capacity). The mass of the hydrated sample should also be recorded.

Pre-measurement desiccation

To desiccate a plant sample, place it on a raised platform (to sit in the headspace above the desiccation agent) such as a 35 × 15-mm Petri dish in a sealed 150-mL desiccation chamber. Use an aqueous salt solution to reach the desired relative humidity (RH) in each chamber. To achieve a consistent headspace RH of 35% ± 5%, we used MgCl dissolved in deionized water. Before placing samples in the desiccation chambers, determine the concentration of MgCl needed for each growth chamber to reach the desired RH. Hygrochron iButtons can be used to monitor the RH inside each chamber, increasing the concentration of MgCl until the desired RH is reached. Sample desiccation may take multiple days, so this should be factored into MgCl calculations.

Infrared gas analysis

During carbon (C) balance data collection, the within-chamber settings for the LI-6800 IRGA should include the following constants: desired reference CO_2 concentration (e.g., ambient), saturating light intensity, moderate RH, medium to high flow rate, and moderate temperature. The settings we used for the current case study included a reference CO_2 concentration of 410 ppm, photosynthetically active radiation (PAR) of 800 $\mu mol \cdot m^{-2} \cdot s^{-1}$ (previously shown to be a saturating, but non-photochemistry-damaging light intensity for *S. caninervis*; Coe et al., 2012), 70% RH, 24°C, and a flow rate of 700 $\mu mol \cdot s^{-1}$. The LI-6800 was programmed to log data every

15 s. Every 10 min, the LI-6800 performed an IRGA matching routine as outlined in the LI-6800 manual to align sample and reference IRGAs and prevent any drift in measurements. All samples were run for at least 12 h to ensure that the entirety of the C balance curve was captured. This cutoff was previously determined to be sufficient to capture C fluxes given the size of the simulated precipitation events (2–4 mL equivalent) delivered.

To isolate the C flux caused exclusively by plant tissue, the potential for C flux caused by the substrate in the sample must be addressed. This protocol involves completing two IRGA curves: one with the plant and substrate together (plant +substrate curve) and one with the plant material removed (substrate-only curve). A final analytical step subtracts the substrate-only curve from the plant+substrate curve, leaving the C flux caused by the plant. Before running IRGA curves, set up the Autolog program to meet your desired data collection frequency (e.g., every 15 s).

To run the plant+substrate curve, place an intact, dry plant sample within the measurement chamber (Figure 2, Figure A4). Initiate the Autolog program, and after several logs of data (e.g., ~1 min if using a measurement frequency of 15 s), use the syringe to slowly (over 10–15 s) administer the calculated saturating water volume (V_p) to the sample (Figure A4). Allow the curve to run for enough time that the plant sample returns to a completely desiccated state (i.e., the carbon flux [A] will be hovering around zero [this could take as long as 12 h]). At this point, the plant+substrate curve is complete.

To run the substrate-only curve on the same sample, remove the dry sample from the LI-6800 chamber and carefully remove the plant material from the substrate. Depending on the size of the plant and the texture of the substrate, you may choose to pre-process the substrate to remove any remaining plant particles. In our case study, once aboveground plant material was removed, the soil was removed from the Petri dish, ground briefly with a mortar

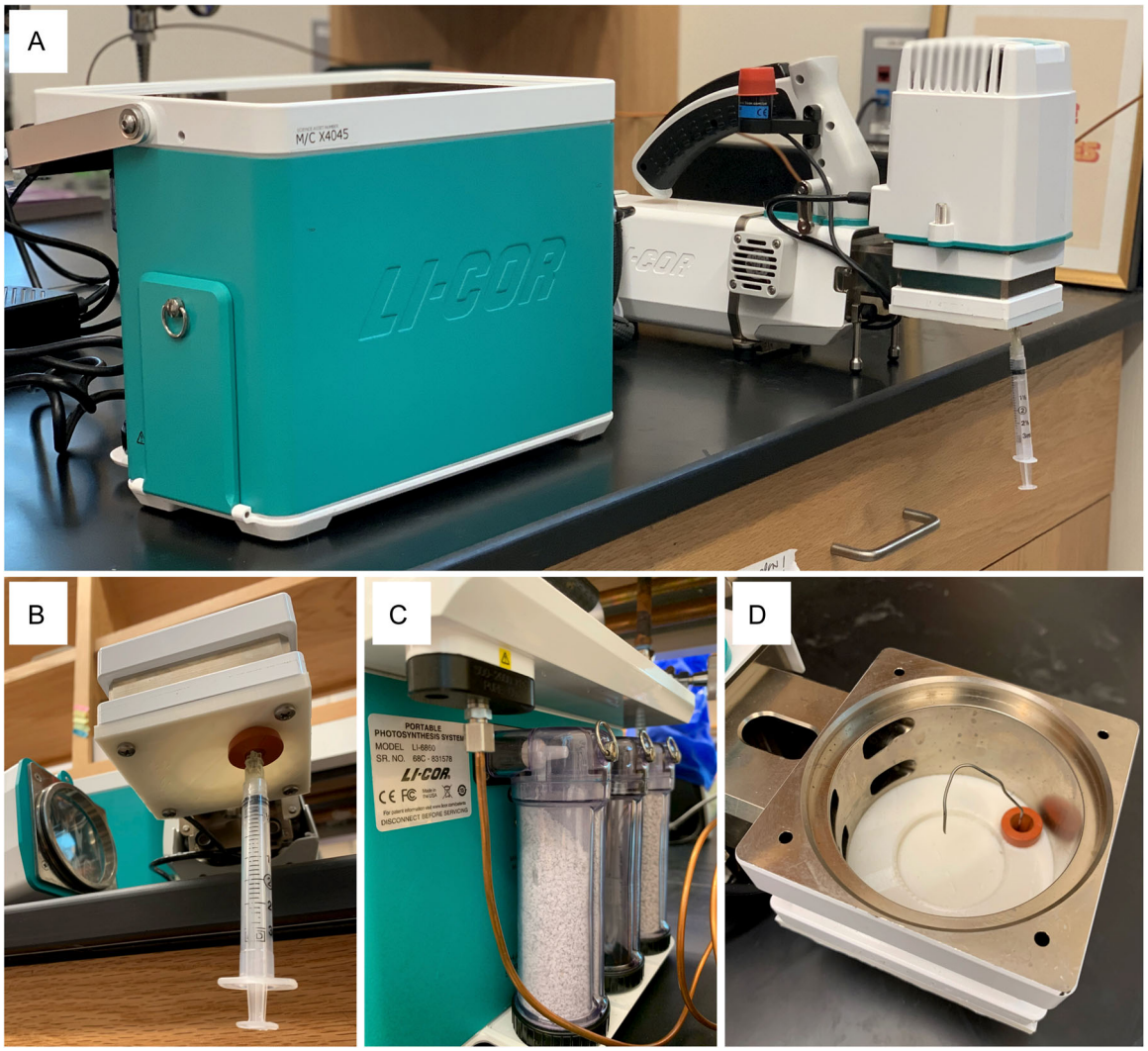

FIGURE A4 Photographs of custom infrared gas exchange system used for carbon balance measurement. (A) Entire setup including the LI-6800 factory system. Note: The external CO_2 tank is out of the frame, to the right of the bench. (B) Syringe-based water delivery system to the sample chamber (view from below). (C) In-line CO_2 delivery using copper tubing. (D) Top view of the plant chamber water delivery system, with the light source removed.

and pestle, and filtered through a 250-micron sieve to remove any remaining pieces of plant tissue. Sample soil was then weighed using a microbalance (Mettler Toledo XS105). Use soil dry mass to calculate the required water for saturation (V_s). Return the substrate material to the Petri dish and place the Petri dish in the LI-6800 measurement chamber to run the substrate-only curve. Run the substrate-only curve in the same manner as the plant+substrate curve, but use V_s instead of V_p.

Instrument testing for water sensitivity

In some cases, the addition of water to samples in a closed system has the potential to influence IRGA measurements in the absence of plant physiological processes. For example, the presence of water vapor can cause instrument cross-sensitivity because both water vapor and CO_2 have infrared light absorption in the same region of the spectrum (4.26 μm wavelength; Kondo et al., 2014), and therefore the analyzer has the potential to detect water vapor as CO_2. To test for this, one can conduct a pilot experiment using an empty (non-sample-containing) 35-mm Petri dish for approximately 12 h (the maximum duration of most C balance data collection periods), and during the measurement period check for overestimation of CO_2 or changes in CO_2 kinetics by the LI-6800 when water is added.